Simulation of recent northern winter climate trends by greenhouse-gas forcing

Drew T. Shindell[1,2], Ron L. Miller[2,3], Gavin A. Schmidt[1,2], and Lionel Pandolfo[4]

[1] NASA Goddard Institute for Space Studies, 2880 Broadway, New York, New York, 10025 USA
[2] Center for Climate Systems Research, Columbia University, New York, New York, 10025 USA
[3] Dept. of Applied Physics, Columbia University, New York, New York, 10027 USA
[4] Dept. of Earth and Ocean Sciences, University of British Columbia, Vancouver, BC V6T 1Z4 Canada

The temperature of air at the Earth's surface has risen during the past century[1], but the fraction of the warming that can be attributed to anthropogenic greenhouse gases remains controversial. The strongest warming trends have been over Northern Hemisphere land masses during winter, and are closely related to changes in atmospheric circulation. These circulation changes are manifested by a gradual reduction in high-latitude sea-level pressure, and an increase in mid-latitude sea-level pressure associated with one phase of the Arctic Oscillation (a hemisphere-scale version of the North Atlantic Oscillation)[2]. Here we use several different climate-model versions to demonstrate that the observed sea-level pressure trends, including their magnitude, can be simulated by realistic increases in greenhouse-gas concentrations. Thus, although the warming appears through a naturally occurring mode of atmospheric variability, it may be anthropogenically induced and may continue to rise. The Arctic Oscillation trend is captured only in climate models that include a realistic representation of the stratosphere, while changes in ozone concentrations are not necessary to simulate the observed

climate trends. The proper representation of stratospheric dynamics appears to be important to the attribution of climate change, at least on a broad regional scale.

While the troposphere has been warming in recent decades, the stratosphere has been steadily cooling[3-5], the strength of the stratospheric jet has been increasing[6], and there are indications that the strength of the polar vortex is also increasing[7]. These trends may be related, as observational studies indicate a dynamical coupling between the lower stratosphere and the troposphere[6-10]. A coupled troposphere/stratosphere mode of internal variability has also been reproduced in climate models[11,12].

It is difficult to determine from observations whether these trends, associated with internal modes of variability, are anthropogenically forced[13,32] or temporary and thus coincidental to the trend in increasing greenhouse-gas concentrations[14]. Climate models can help to distinguish between these possibilities. Here we present the response of a number of climate models to an increase in greenhouse-gas concentrations. Each model is based upon the NASA Goddard Institute for Space Sciences (GISS) atmospheric General Circulation Model[15-17], and is described in Table 1 and Fig. 1. Briefly, the stratospheric models SC, SG, and SO are respectively a control simulation, a simulation with greenhouse-gas forcing, and a simulation with polar ozone and greenhouse gases. The tropospheric models T8G and T4G are greenhouse-gas forcing simulations. Both versions have a low model top compared with the stratospheric models, while T4G has higher horizontal resolution.

Interannual variability of Northern Hemisphere wintertime sea-level pressure (SLP) in both the observations and models is dominated by a nearly axisymmetric spatial pattern centered over the Arctic, as shown by the leading Empirical Orthogonal Function (EOF)[18] in Fig. 2a-c. This observed pattern is defined as

the Arctic Oscillation (AO)[2]. The classic North Atlantic Oscillation contrast between midlatitude and high-latitude SLP is reproduced in the models (Fig. 2b-c) although the observed structure in the North Pacific area is less evident[19].

There is a trend towards decreasing high-latitude SLP and increasing mid-latitude SLP in the stratospheric models (SG, SO; Fig. 2b) that mirrors the rise in globally-averaged model temperature (Fig. 1) and which resembles the observed SLP trends of recent decades. Following Thompson and Wallace[2], we define the time series corresponding to the leading EOF (Fig. 2b) as the 'index' of the model's AO. A linear fit to the AO index has a slope significantly different from zero (Table 1), and the magnitude of the trend (~0.8 mbar per decade over 50 years, starting after 20 years of forcing) resembles the observed value (~1 mbar per decade over the past 30 years). Interdecadal variability is large, and the AO trend might be overlooked were the simulation not extended beyond the initial few decades. The AO index exhibits little additional increase in the final decades of the simulation, despite the continued increase in greenhouse forcing and surface air temperature.

We find that the observed wintertime SLP trend is reproduced only by models that resolve stratospheric dynamics (Fig. 2b). In contrast, models lacking a dynamical stratosphere (including T8G and T4G) uniformly fail to simulate the observed trend in the AO, even though this mode is present and dominates the wintertime variability of each model (Fig. 2c). A greater surface warming at high latitudes, the typical response of a general circulation model to increasing GHGs[11,15-17,20], does lead to decreased SLP in the Arctic relative to mid-latitudes over time, but these changes are only weakly correlated with the AO. In fact, the trend of the AO time series is not statistically distinct from zero in either tropospheric model (Table 1). Although these models contain two dynamical layers above the tropopause, this is insufficient to resolve stratospheric dynamics.

The inability of these tropospheric models to produce an AO trend is not affected by changes in horizontal resolution, physical parameterizations or the ocean component. This behavior suggests that stratospheric dynamics must be accounted for in the problems of detection and prediction of future warming.

Observed interannual variations in stratospheric circulation are well-correlated with the AO[2], and this relationship is reproduced by the stratospheric models. Fig. 2d shows the leading EOF of 30-mbar geopotential height in model SG. The corresponding time variation has a high correlation with the AO index, irrespective of whether each field is first detrended, on both interannual and multi-decadal time scales. A reduction in Arctic SLP is associated with a deepening of the stratospheric polar vortex and a strengthening of the polar night jet.

Polar ozone depletion is a candidate for driving observed stratospheric trends[2,20,21], which are correlated with the AO index. However, the simulation SG, where ozone changes are absent, exhibits the same increase in the AO index as SO, where polar ozone chemistry is calculated through an interactive photochemical parameterization[22]. To identify the effect of ozone forcing, EOFs of wintertime SLP (for simulation SO) were recalculated for two separate periods: December and January versus March and April. Although ozone forcing is largest during the latter period, the multi-decadal trend in the AO index, evident in Fig. 2b, is present only in the December to January variability. This result, along with the nearly identical AO trends in models SO and SG, suggests that ozone forcing is not necessary to increase the AO index or to strengthen the stratospheric polar vortex.

In addition to its connection to the stratosphere, the AO index is correlated with the recent rise in Northern Hemisphere land temperatures that is cited as evidence of anthropogenic warming[23,24]. The decrease in high-latitude SLP and

increase in mid-latitude SLP is associated with increased wintertime advection of relatively warm oceanic air across northern Asia, causing a local rise in temperature[2]. Similarly, onshore advection warms North America, and the temperature falls in the vicinity of the Bering Strait and the eastern Canadian Arcitc owing to the offshore flow of cold continental air.

To examine the relationship between the AO index and surface air temperature, we detrended both fields and regressed the former upon the latter. Detrending is used to remove any spurious correlation that might arise from the trend in both time series. The observed regression pattern (Fig. 3a) is reproduced by all models. Figure 3b and c show the regression pattern in the stratospheric and tropospheric models, SG and T8G, respectively. A strengthened zonal circulation (corresponding to an increased AO index) is associated with a region of anomalously warm temperature extending from Europe across northern Asia. In addition, cold anomalies are present in the vicinity of the Bering Strait and Labrador. Neither the warm nor the cold anomalies are as extensive as the observed pattern, although better agreement is exhibited by models with higher horizontal resolution (not shown). A comparison of the observed and modelled surface warming is made difficult by the absence of aerosol changes and dynamic ocean feedbacks in these models. In addition, the model trends are estimated over a longer period than the observations, increasing their signal-to-noise ratio. However, Fig. 3d-f suggests that models reproducing the observed AO trend will exhibit enhanced wintertime warming over northern Eurasia as observed.

In the stratospheric models, increasing greenhouse gases have a significant influence on the propagation of planetary waves from the troposphere into the stratosphere[12,22]. The latitudinal temperature gradient near the tropopause increases as the tropics and mid-latitudes warm, while the high latitudes cool, enhancing the zonal wind at these levels. This results in a deflection of high-

latitude wave energy away from the lower stratosphere. The zonally-averaged vertical circulation is then enhanced, with greater rising motion in the polar latitudes and descent between 40° and 55°N, continuously from the surface to the middle stratosphere, in accord with the deep barotropic nature of the AO (ref. 2). This results in a cooling northward of about 55°N, and a warming at lower latitudes, and a corresponding increase in the westerly zonal wind around 55°N from the surface up to about the 1-mbar level. The net result is a strengthened polar vortex aloft, while the enhanced zonal circulation at the surface leads to a greater advection of warm air onto land, and of cold air over the oceans. Thus stratospheric dynamics modulates the propagation of tropospheric energy, in addition to altering stratospheric energy itself. The influence of the stratosphere on the troposphere is consistent with the observed co-variability between the two levels[2]. Furthermore, a recent analysis shows that, on average, the observed AO signature propagates downwards from the stratosphere reaching the surface after ~3 weeks (M. Baldwin and T. Dunkerton, personal communication).

The GISS stratospheric models are distinguished from their 'tropospheric' counterparts by their ability to generate a realistic climatology in the stratosphere. This is influenced by the higher upper boundary (0.002 mbar versus 10 mbar), greater vertical resolution above the tropopause, and the inclusion of different physics (for example, gravity wave drag), among other factors. Other general circulation models also show a trend in the AO index in response to increasing greenhouse gases (ref. 20 and R.McDonald, personal communication). However, the trends are weaker than those seen in the GISS stratospheric models or in the observations. These general circulation models, like the GISS tropospheric models, have only limited representations of the stratosphere. An upper boundary in the middle stratosphere (~5-10 mbar) limits a model's ability to properly simulate planetary wave propagation[12,25,26], which might affect the

models' ability both to produce an overall AO trend and to reproduce how the total SLP trend projects upon the AO.

The spatial structure of the Arctic Oscillation is reproduced as the leading wintertime mode of Northern Hemisphere SLP in all the GISS models studied. Furthermore, an increase in the AO index consistent with the recent observed trend occurs in response to anthropogenic greenhouse gases in models containing stratospheric dynamics. This suggests that the observed trend is a signature of anthropogenic greenhouse gases and that trends in surface air temperature associated with the AO should be attributed to human activities, rather than to natural variability. Thus, greenhouse gases may induce climate change through dynamical effects, in addition to direct radiative forcing. Despite the absence of ozone forcing in one stratospheric model, both models exhibit strengthening of the stratospheric polar vortex in association with the decrease in Arctic SLP, suggesting that ozone is not fundamental to the observed trend. The failure of tropospheric models to reproduce the observed AO trend suggests that stratospheric dynamics are crucial to certain important aspects of tropospheric variability, at least in the models analysed here. As changes in SLP are associated with anomalies in surface air temperature, the inclusion of stratospheric dynamics in a model may be fundamental to the simulation of present warming, along with the prediction of future climate change. Although hemispherically averaged warming associated with the AO trend is a small component of the total, it has a distinct regional signal which may be important for detection of the anthropogenic influence on surface air temperatures. There may be many ways to excite the AO. Detection and attribution of the effect of a change in the AO will probably depend on proper simulation of the dominant mechanisms governing its behavior.

We suggest that the stratosphere influences climate at the surface by

modulating energy propagation out of the troposphere. This mechanism implies that changes to the stratosphere, whether induced by variations in greenhouse gases, solar flux, ozone, or volcanic forcing[21,27,28], may all affect surface climate. It remains unclear whether, and through what mechanism, the AO trend saturates towards the end of the simulation (Fig. 2b), despite the continued increase in forcing and surface air temperature. Perhaps the stratospheric polar vortex has strengthened and stabilized to such an extent that virtually all planetary waves are refracted away. The relative importance of the various factors influencing the quality of the model's stratospheric simulation (for example, the height of the model's upper boundary, the vertical resolution above the tropopause) will become clearer with further study. An Antarctic counterpart to the AO trend is also exhibited by both stratospheric models, with amplitude comparable to Arctic values. Such a trend has recently been identified in the observations[29].

1. J. Hansen, R. Ruedy, M. Sato, and R. Reynolds, Global surface air temperature in 1995: Return to pre-Pinatubo level, Geophys. Res. Lett., 23:1665-1668, 1996.

2. D. W. J. Thompson and J. M. Wallace, The Arctic Oscillation signature in the wintertime geopotential height and temperature fields, Geophys. Res. Lett, 25:1297-1300, 1998.

3. A. H. Oort and H.-Z. Liu, Upper-air temperature trends over the globe, J. Clim., 6:292-307, 1993.

4. R. W. Spencer and J. R. Christy, Precision lower stratospheric temperature monitoring with the MSU: Technique, validation, and results 1979--1991, J.

Clim., 6:1194-1204, 1993.

5. S. Pawson, K. Labitzke, and S. Leder, Stepwise changes in stratospheric temperature, Geophys. Res. Lett., 25:2157-2160, 1998.

6. K. Kodera and H. Koide, Spatial and seasonal characteristics of recent decadal trends in the Northern Hemisphere troposphere and stratosphere, J. Geophys. Res., 102:19433-19447, 1997.

7. R. W Zurek, G. L. Manney, A. J. Miller, M. E. Gelman, and R. M. Nagatani, Interannual variability of the north polar vortex in the lower stratosphere during the UARS mission, Geophys. Res. Lett., 23:289-292, 1996.

8. M. P. Baldwin, X. Cheng, and T. J. Dunkerton, Observed correlations between winter mean tropospheric and stratospheric circulation anomalies, Geophys. Res. Lett., 21:1141-1144, 1994.

9. J. Perlwitz and H-F. Graf, The statistical connection between tropospheric and stratospheric circulation of the Northern Hemisphere in winter, J. Clim., 8:2281-2295, 1995.

10. K. Kodera, M. Chiba, H. Koide, A. Kitoh, and Y. Nikaidou, Interannual variability of the winter stratosphere and troposphere in the Northern Hemisphere, J. Met. Soc. Jpn, 74:365-382, 1996.

11. A. Kitoh, H. Koide, K. Kodera, S. Yukimoto, and A. Noda, Interannual variability in the stratosphere-troposphere circulation in a coupled ocean-

atmosphere GCM, Geophys. Res. Lett., 23:543-546, 1996.

12. D. Rind, D. Shindell, P. Lonergan, and N. K. Balachandran, Climate change and the middle atmosphere. Part III: The doubled CO2 climate revisited, J. Clim., 11:876-894, 1998.

13. T. N. Palmer, A nonlinear dynamical perspective on climate change, Weather, 48:314-326, 1993.

14. J. W. Hurrell, Influence of variations in extratropical wintertime teleconnections on Northern Hemisphere temperature, Geophys. Res. Lett., 23:665-668, 1996.

15. J. Hansen et al., Efficient three-dimensional global models for climate studies: Models I and II, Mon.Wea.Rev., 111:609-662, 1983.

16. D. Rind, R. Suozzo, N. K. Balachandran, A. Lacis, and G. Russell, The GISS global climate/middle atmosphere model. Part I: Model structure and climatology, J. Atmos. Sci., 45:329-370, 1988.

17. G. L. Russell, J. R. Miller, and D. Rind, A coupled atmosphere-ocean model for transient climate change, Atmosphere-Ocean, 33(4):683-730, 1995.

18. C. S. Bretherton, C. Smith, and J. M. Wallace, An intercomparison of methods for finding coupled patterns in climate data, J. Clim., 5:541-560, 1992.

19. J. M. Wallace and D. S. Gutzler, Teleconnections in the geopotential height

field during the Northern Hemisphere winter, Mon.Weather Rev., 109:784-812, 1981.

20. H-F. Graf, I. Kirchner, and J. Perlwitz, Changing lower stratospheric circulation: The role of ozone and greenhouse gases, J. Geophys. Res., 103:11,251-11,261, 1998.

21. E. M. Volodin and V. Galin, Interpretation of winter warming at Northern Hemisphere continents 1977-94, J. Clim., in press, 1999.

22. D. T. Shindell, D. Rind, and P. Lonergan, Increased polar stratospheric ozone losses and delayed eventual recovery due to increasing greenhouse gas concentrations, Nature, 392:589-592, 1998.

23. J. M. Wallace, Y. Zhang, and L. Bajuk, Interpretation of interdecadal trends in Northern Hemisphere surface air temperature, J. Clim., 9:249-259, 1996.

24. A. J. Broccoli, N. C. Lau, and M. J. Nath, The cold ocean warm land pattern: Model simulation and relevance to climate change detection, J. Clim., 11:2743-2763, 1998.

25. B. A. Boville and X. Cheng, Upper boundary effects in a general circulation model, J. Atmos. Sci., 45:2591-2606, 1988.

26. J. Austin, N. Butchart, and R. S. Swinbank, Sensitivity of ozone and temperature to vertical resolution in a GCM with coupled stratospheric chemistry, Q. J. R. Met. Soc., 123:1405-1431, 1997.

27. D. T. Shindell, D. Rind, N. Balachandran, J. Lean, and P. Lonergan. Solar cycle variability, ozone, and climate. Science, 284, 305-308, 1999.

28. K. Kodera. On the origin and nature of interannual variability of the winter stratospheric circulation in the Northern Hemisphere. J. Geophys. Res., 100: 14,077-14,087, 1995.

29. D. Gong and S. Wang, Definition of Antarctic oscillation index, Geophys. Res. Lett., 26:459-462, 1999.

30. G. R. North, T. L. Bell, R. F. Cahalan, and F. J. Moeng, Sampling errors in the estimation of empirical orthogonal functions, Mon. Wea. Rev., 110:699-706, 1982.

31. C. Rosenzweig et al., Building linkages among climate, impacts, and economics: a multi-dimensional approach to integrated assessment, Columbia Earth Institute & NASA GISS, New York, NY, 1998.

32. S. Corti, F. Molteni, and T. N. Palmer, Signature of recent climate change in frequencies of natural atmospheric circulation regimes, Nature, 398, 799-802, 1999.

Acknowledgments We thank J. Hansen, D. Rind, and G. Russell for making available their numerical experiments, D. Thompson for providing analyses of the observations and P. Lonergan for assistance with model output. We also thank P. Stone, J. M. Wallace, and an anonymous reviewer for their comments on

earlier drafts of this paper. GAS was supported by a NOAA Postdoctoral Fellowship in Climate and Global Change administered by the UCAR Visiting Scientist Program. RLM is supported by the NOAA Atlantic Climate Change Program. Stratospheric modeling at GISS is supported by the NASA Atmospheric Chemistry Modeling and Analysis Program.

Correspondence and requests for materials should be addressed to D.T.S. (e-mail: dshindell@giss.nasa.gov).

Table 1: Model descriptions and results.

Model	Resolution (L=levels)	Model Top mb (km)	Ocean	Length (years)	Forcing	Slope (mb/decade)	r^2	Ref.
SC	8° × 10°, 23 L	0.002 (85)	ML	89	control	0.03 ± 0.19	0.06	22
SG	8° × 10°, 23 L	0.002 (85)	ML	111	GHG	0.32 ± 0.10	0.27	22
SO	8° × 10°, 23 L	0.002 (85)	ML	111	GHG + O_3	0.31 ± 0.09	0.30	22
T8G	8° × 10°, 9 L	10 (30)	ML	111	GHG	0.03 ± 0.08	0.01	31
T4G	4° × 5°, 9 L	10 (30)	OGCM	110	GHG	0.10 ± 0.12	0.03	17

ML is a mixed-layer ocean with diffusion into the deep ocean and fixed ocean heat transport, while OGCM is a fully coupled dynamic ocean. SG and SO were initialized at the end of the control integration SC. All the models were forced with an increasing greenhouse-gas concentration based on observations from 1959 to 1984, after which an increase similar to the IPCC projection IS92a was used[22]. Aerosol concentrations were constant in all simulations. The slope is the linear least-squares fit to the leading principle component of wintertime Northern Hemisphere SLP (compare Fig. 2) over the entire length of the simulations (except for SC, where the first 20 years of spin-up are discarded). The error estimate corresponds to the 95% confidence level, assuming as a null hypothesis that the detrended time series of successive wintertime values is a first order auto-regressive process.

Figure 1: Global annual-average surface temperature anomalies (°C). The model simulations are described in Table 1.

Figure 2: Northern Hemisphere wintertime climate trends. Shown are the leading

EOF (left panel) and principal component (PC; right panel) of wintertime (November-April) Northern Hemisphere sea-level pressure (SLP) for a) the observations[2], b) the stratospheric model SG (with similar results for SO), c) the tropospheric model T8G, and d) the leading EOF and PC of wintertime (November-April) Northern Hemisphere 30-mbar geopotential height (m) for the stratospheric model SG. EOFs are a representation of a data set by a number of fixed spatial patterns, each multiplied by a time-varying amplitude (the PC). The patterns are derived by maximizing the variance corresponding to the pattern multiplied by its PC[18,30]. In each case, the leading mode is statistically well-separated from succeeding modes whether or not SLP is first detrended. Whereas EOFs and PCs are calculated using the individual months, the PC is plotted as a wintertime average. The PCs are scaled to have units of mbar and the spatial pattern has unit amplitude poleward of 60°N. The red curve represents smoothing of the PC by a 10-year tapered running mean. The first EOF in each case explains a) 22%, b) 13%, c) 9%, and d) 53%, respectively of the variance.

Figure 3: Surface air temperature (SAT) and the Arctic Oscillation (AO). Top row, regression of the AO index upon surface air temperature (°C) for a) the observations (ref. 2) (yellow denotes no data), b) the stratospheric model SG and c) the tropospheric model T8G. Bottom row, linear trend (°C per decade) in wintertime (November-April) surface air temperature for d) the observations, e) the stratospheric model SG and f) the tropospheric model T8G. The equivalent plots for the stratospheric model SO are very similar to that for SG.

Shindell et al. 1999
Figure 1.

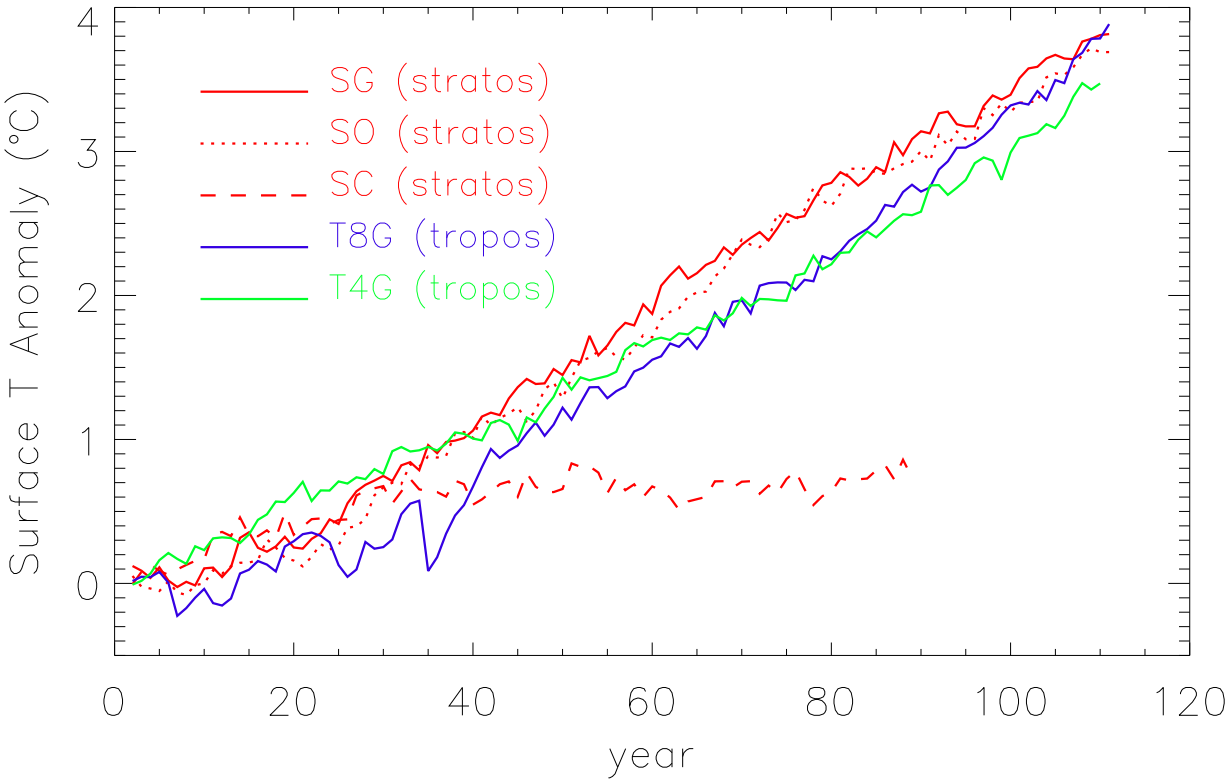

Shindell et al. 1999. Figure 2.

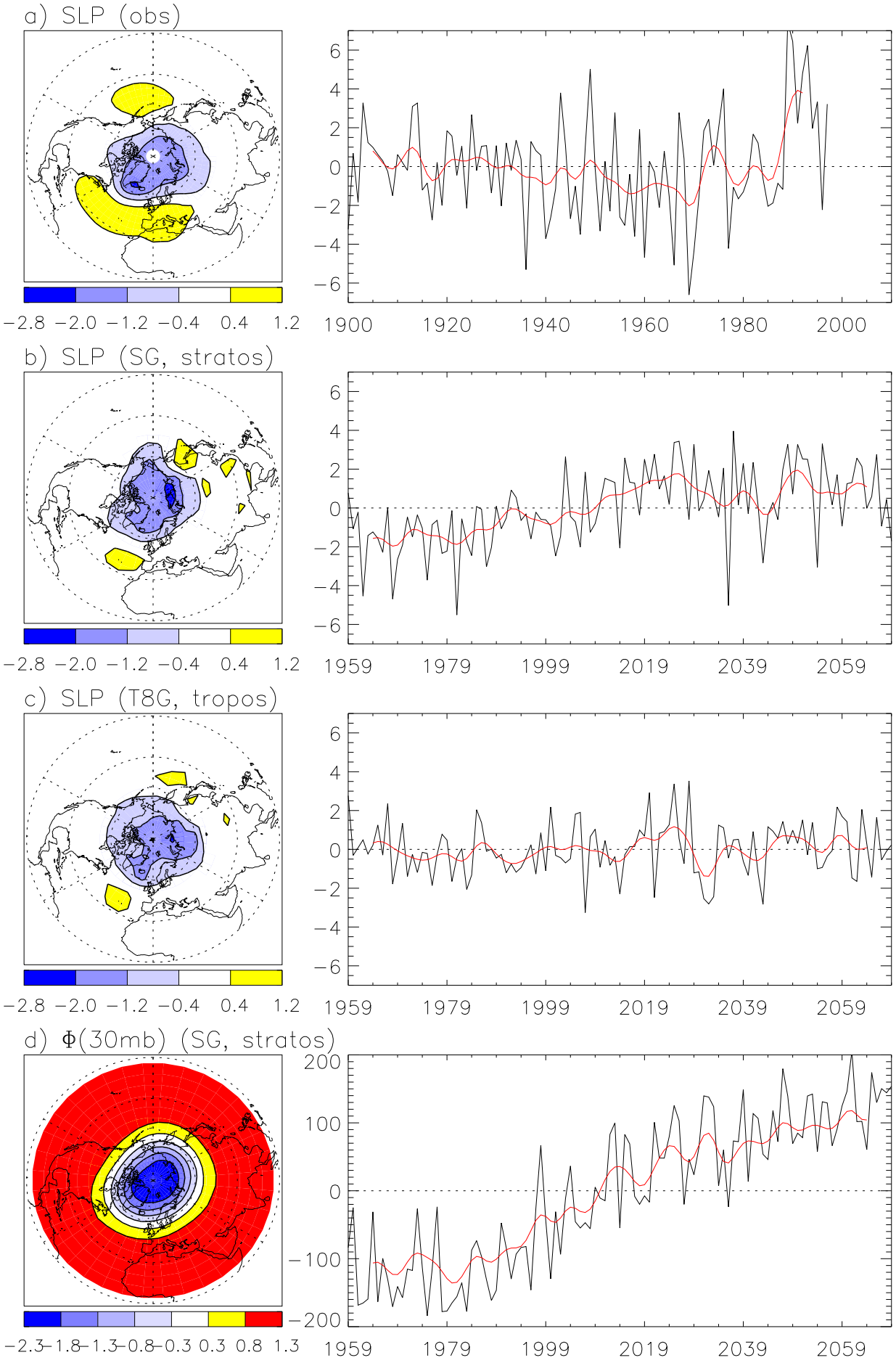

Shindell et al. 1999
Figure 3.